

Strangeness in ALICE at the LHC

Francesca Bellini* for the ALICE Collaboration

*Dipartimento di Fisica dell'Università di Bologna, Via Irnerio 46 - 40126 Bologna (Italy)

E-mail: fbellini@cern.ch

Abstract. Strangeness production has been measured by the ALICE experiment in different collision systems at the unprecedented center-of-mass energies available at the CERN Large Hadron Collider. In Pb–Pb collisions at $\sqrt{s_{NN}} = 2.76$ TeV the relative production of strange and multi-strange baryons relative to pions is observed to follow a saturating trend with increasing centrality, and reaching values that are consistent with those predicted by thermal model calculations in the Grand-Canonical ensemble. More recently, the multiplicity dependence of strangeness production in small systems such as pp and p–Pb has also been investigated. An overview of the most recent results on strangeness production is reported, including the first observation of strangeness enhancement with charged particle multiplicity in pp collisions.

1. Introduction

The study of strangeness production has had a central role in heavy-ion physics since the observation of its enhancement in heavy-ion collisions (A–A) with respect to proton-proton (pp) collisions. This observation was predicted as one of the signatures of the formation of the Quark Gluon Plasma (QGP) [1]. The enhancement, as quantified by comparing the particle yields per participant nucleon pair in A–A collisions to the yields in pp, was measured at SPS and RHIC and finally by ALICE at the LHC, where it was soon clear that a key ingredient for a proper interpretation of the results is the understanding of the evolution of strangeness production in the reference pp collisions with the collision energy. Since the average number of charged particles does not scale linearly with the average number of nucleons participating in the collision, the ratio of strange particle yield to pion yield is used to quantify the enhancement of strangeness production.

Recently, ALICE has performed measurements in pp and proton-lead (p–Pb) collisions to investigate strangeness production as a function of the charged-particle multiplicity. This effort is part of a growing interest of the heavy-ion community in the detailed study of the dynamics of small systems, after the observation by the LHC experiments of features in pp and p–Pb collisions traditionally associated with the presence of a QGP in Pb–Pb collisions and hinting at the presence of collective phenomena [2, 3].

This work is intended as a brief review of the new ALICE results on identified particle production presented at this conference, with a focus on two key topics that are presently subject of animated discussions in the community: the investigation of features associated to collectivity-driven in small systems and the multiplicity-differential measurements of strangeness production in pp.

2. Production of identified hadrons in pp, p–Pb and Pb–Pb

ALICE has measured the production of a large variety of identified particles¹, including pions, kaons and protons, strange and multi-strange hadrons (K_S^0 , Λ , Ξ , Ω), short-lived hadronic resonances ($\rho(770)^0$, $K^*(892)^0$, $\phi(1020)$, $\Sigma(1385)^\pm$, $\Xi(1530)^0$), and light nuclei (d, ^3H , ^3He , ^4He), in proton-proton (pp), proton-lead (p–Pb) and lead-lead (Pb–Pb) collisions. The yields of a selection of these particles relative to pions are reported in figure 1 as a function of the average charged particle multiplicity density at midrapidity ($|\eta| < 0.5$), $\langle dN_{\text{ch}}/d\eta \rangle$.

The reader can refer to [4] for details on the ALICE sub-detectors and their particle identification performance. For the measurements presented in this work, the forward-rapidity array scintillator counters V0A and V0C, and the T0 system have been used for triggering and background rejection. In order to avoid auto-correlation biases, events are classified in centrality in Pb–Pb and multiplicity in pp and p–Pb collisions, based on the total charge deposited in the forward V0A and V0C detectors. The values of $\langle dN_{\text{ch}}/d\eta \rangle$ for each event class are measured at midrapidity. $\langle dN_{\text{ch}}/d\eta \rangle$ spans over three orders of magnitude in Pb–Pb collisions (up to $O(10^3)$), while it ranges from few units to few tens in pp and p–Pb collisions, with a significant overlap between the two systems. The Inner Tracking System (ITS) and the Time Projection Chamber (TPC) are used for vertexing, tracking and particle identification (PID). The Time-Of-Flight (TOF) system and the High Momentum Particle Identification (HMPID) detector allow to extend the range of identification for charged particles and light nuclei to higher momentum. In addition, the topological reconstruction of weak decays is exploited to identify strange and multi-strange particles. Thanks to the combination of different PID techniques, ALICE is able to identify hadrons with momenta between 150 MeV/c and 20 GeV/c.

The centrality-dependent transverse momentum (p_T) spectra of pions, kaons and protons in Pb–Pb collisions at $\sqrt{s_{\text{NN}}} = 2.76$ TeV have been published recently in [5] together with their nuclear modification factors R_{AA} , defined as the ratio of the yield in Pb–Pb collisions to the pp yield scaled by the number of binary collisions. In figure 2 the preliminary measurements of the Ξ and Ω R_{AA} in central Pb–Pb collisions are compared to the modification of inclusive

¹ For brevity, the notation for particles is used in these proceedings to indicate both particles and antiparticles, and resonance masses will be omitted.

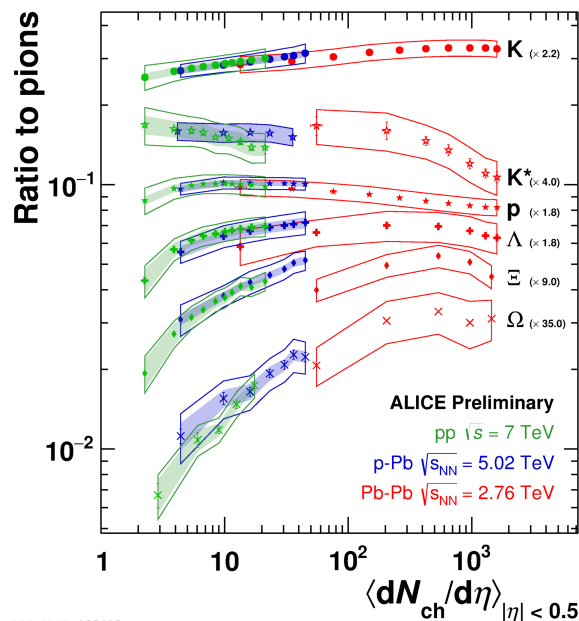


Figure 1. Yield of K , K^{*0} , p , ϕ , Λ , Ξ , Ω relative to the pion yield as a function of $\langle dN_{\text{ch}}/d\eta \rangle$ measured at midrapidity ($|\eta| < 0.5$) in pp, p–Pb, Pb–Pb collisions.

charged particles, π , K, p, ϕ and the average R_{AA} of D-mesons. A strong suppression at high p_T ($p_T > 8$ GeV/c) is observed for all particle species under study, including open-charm mesons, suggesting that the mechanism responsible for the suppression is flavour-independent. In the low and intermediate p_T range several effects can result in the difference observed in both the shapes and maxima of the distributions: the presence of radial flow in Pb–Pb collisions shifts the maxima of the spectra towards higher values according to the mass of the particle; the strangeness content might cause the enhancement of the R_{AA} of Ω above 1; the significantly different reference spectra of p and the ϕ -meson in pp collisions justifies the difference in the R_{AA} at $2 < p_T < 4$ GeV/c of these particles, whose ratio of spectra in Pb–Pb collisions is flat in the same p_T range [6].

The analysis of two small data samples of pp and Pb–Pb collisions at $\sqrt{s_{NN}} = 5.02$ TeV collected in late 2015 and corresponding to 3% and 25% of the available statistics, respectively, has led to a preliminary measurement of the R_{AA} of inclusive charged particles at the new energy. The measurement exploits an improved analysis technique that allows to reduce significantly the systematic uncertainty on the spectra with respect to the 2.76 TeV case [7]. The R_{AA} of charged particles at 5.02 TeV is reported in figure 3 for six different centrality intervals and compared to the previous measurement at 2.76 TeV. Particle production at high p_T is increasingly suppressed from peripheral to central events, where the suppression is consistent with the observations at 2.76 TeV. Since a hardening of the spectra is expected for increasing $\sqrt{s_{NN}}$, this observation may indicate a larger parton energy loss in a hotter and/or denser medium produced at the higher energy. A new analysis of the 2.76 TeV data is in progress with the same improved analysis technique used at 5.02 TeV in order to allow a more precise comparison of the two energies, especially for the 40-60% and 60-80% centrality classes, where some hints for differences at $p_T > 5$ GeV/c can be noted, yet within the current systematic uncertainties.

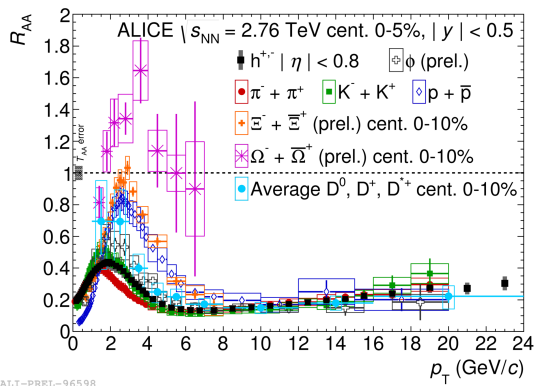
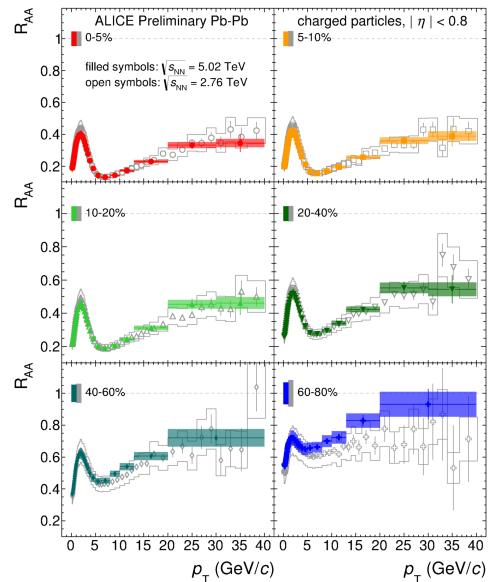


Figure 2. R_{AA} for various particle species in central Pb–Pb collisions at $\sqrt{s_{NN}} = 2.76$ TeV.



ALI-PREL-107300

Figure 3. R_{AA} of inclusive charged particles in central Pb–Pb collisions at $\sqrt{s_{NN}} = 5.02$ TeV.

Similarly to Pb–Pb, no flavour dependence is observed at high- p_T for the nuclear modification factor R_{pPb} in p–Pb collisions at $\sqrt{s_{NN}} = 5.02$ TeV [8]. The R_{pPb} of π , K, p is consistent with unity above $p_T \sim 8$ GeV/ c , indicating that the suppression observed in central Pb–Pb collisions is due to parton energy loss in the medium created in the collision. At intermediate p_T (2 to 6 GeV/ c), where also Ξ and Ω can be added to the picture [9], the Cronin peak exhibits mass ordering, reminiscent of the mass ordering observed for the $\langle p_T \rangle$ [10].

3. Searches for collectivity in small systems

The role of radial flow and particle production mechanisms (fragmentation, recombination) in defining the spectral shapes in the intermediate- p_T range can be investigated by studying baryon-to-meson (B/M) ratios. Ratios of particles with a large mass difference, such as p/π and Λ/K_S^0 , or, on the contrary, with very similar masses such as p/ϕ , are good candidates in this respect. The comparison of the $\sqrt{s_{NN}} = 2.76$ TeV Pb–Pb results with theoretical models have shown that a good agreement with data is achieved over a broad p_T range when hydrodynamics is taken into account, as done in EPOS [11], thus suggesting that the so-called “baryon anomaly” observed in central Pb–Pb collisions may be a consequence of a strong radial flow. In addition, it was shown that models of parton recombination can also describe the data [12]. The p/π and Λ/K_S^0 ratios have been measured as well in pp at 7 TeV and p–Pb at 5.02 TeV for various event classes [13]. Both ratios exhibit a depletion at low p_T and an enhancement at intermediate p_T going from low to high multiplicity within each system. Although the magnitudes of the depletion and enhancement are different across different systems, the similarity with the Pb–Pb case is striking. Is this an indication for the presence of collectivity in small systems?

In order to try to answer this question, the transverse momentum spectra of pions, kaons and protons in both pp and p–Pb have been fitted simultaneously with a Blast-Wave function [14], as done for the Pb–Pb case [15]. For each multiplicity class the fitting range is optimised in order to ensure a $\chi^2/\text{ndf} < 1$. Then the fit is used to quantify the freeze-out parameters and the evolution of the system with centrality in the $T_{kin} - \langle \beta_T \rangle$ plane, where T_{kin} represents the kinetic freeze-out temperature and β_T the radial expansion velocity. In this picture, radial velocity increases while the freeze-out temperature decreases with increasing centrality in Pb–Pb. The resulting fit parameters are reported for the three systems in figure 4. The evolution with multiplicity is similar in pp and p–Pb, but at similar multiplicities the smaller system exhibits a larger β_T . In p–Pb the fit to the highest-multiplicity class π , K and p spectra returns parameters that can also describe the Ξ and Ω spectra, contrary to what happens in Pb–Pb collisions [9]. In pp collisions, despite still large uncertainties on the parameters of the fit, Ξ and Ω spectra can also be described fairly well by the Blast-Wave model. The Blast-Wave fit to particle spectra is increasingly being used as a tool to search for radial flow-like collectivity. However some caution has to be applied in the interpretation of the results, especially when comparing the results of the fit across different systems or experiments, where the sensitivity to the fitting range may play a role. Moreover, it has to be noted that mechanisms such as Color Reconnection [16], as implemented in the PYTHIA8 event generator [17], can mimic the effects of a collective radial expansion. Finally, the spectra of resonances seem not to be successfully predicted by using the parameters from the simultaneous Blast-Wave fit to long-lived hadrons.

Short-lived resonances decay very early, with lifetimes that are of the same order of magnitude as the hadronic phase in Pb–Pb collisions. Only the ϕ p_T spectrum is satisfactorily described by the Blast-Wave model in central Pb–Pb collisions [6], whereas the model overshoots the yield of K^{*0} at low p_T . This is presently interpreted as an effect of re-scattering in the hadronic phase. Re-scattering effects of resonances are expected to be stronger in central Pb–Pb collisions, where the medium is denser and longer lived, and to affect predominantly the low momentum part of the spectrum ($p_T < 2$ GeV/ c [18]). This is reflected in the suppression observed for the p_T -integrated yield ratios of K^{*0}/K and ρ^0/π going from peripheral to central Pb–Pb [19]. K^{*0} and

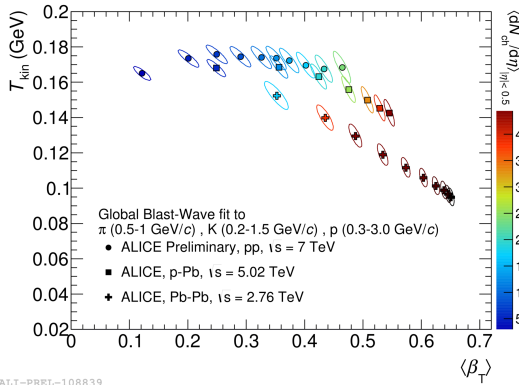


Figure 4. Blast-Wave parameters resulting from the simultaneous fit of identified particle spectra in pp, p-Pb and Pb-Pb collisions in various multiplicity or centrality bins. Colors indicate the scale in multiplicity.

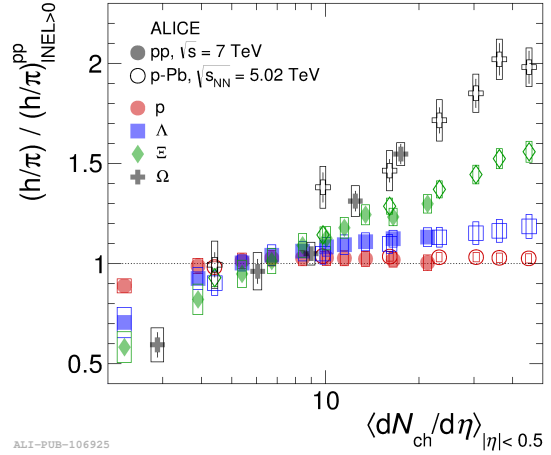


Figure 5. Particle yield relative to pion in pp at $\sqrt{s} = 7$ TeV and p-Pb at $\sqrt{s_{NN}} = 5.02$ TeV as a function of the average charged particle multiplicity, normalised to the same ratio in multiplicity-integrated pp (INEL>0).

ρ^0 are indeed about ten times shorter-lived than the ϕ , whose ratio to K shows no significant variation over centrality. The decreasing trend of both resonances is qualitatively reproduced by the EPOS3 event generator when the core-corona development of the fireball is followed by a hadronic afterburner phase modelled via UrQMD [20]. Recent measurements of the K^{*0}/K ratio in p-Pb and pp (see figure 1) also hint at the presence of a decreasing trend with multiplicity, although not significant given the present uncertainties.

4. Strangeness production in pp, p-Pb and Pb-Pb

The ratios of strange and multi-strange hadron production relative to pions in pp at $\sqrt{s} = 7$ TeV, p-Pb at $\sqrt{s_{NN}} = 5.02$ TeV and Pb-Pb at $\sqrt{s_{NN}} = 2.76$ TeV are reported in figure 1 as a function of $\langle dN_{ch}/d\eta \rangle$. In Pb-Pb the ratios follow a rather constant behaviour, saturating to values that are consistent with those predicted by Grand-Canonical thermal models [21, 22]. In pp and p-Pb, Ξ/π and Ω/π increase from low to high multiplicity events to values consistent with those measured in central and peripheral Pb-Pb collisions, respectively. A similar behaviour with multiplicity is observed in p-Pb for the resonant state of Ξ in the Ξ^{*0}/π ratio, suggesting that the strangeness content of the hyperon drives the increase and dominates over possible mass effects. A comprehensive set of measurements in pp collisions at $\sqrt{s} = 7$ TeV [23] shows that while Λ/K_S^0 and p/π do not increase significantly, the Ξ/π and Ω/π increase with multiplicity following a trend compatible with that in p-Pb collisions across the same range of multiplicity. The comparison with other non-strange identified-particle ratios, such as the p/π ratio or Λ/K_S^0 can help in understanding if the increase is related to mass or to strangeness content. Both ratios are found flat with multiplicity. Figure 5 shows the pp and p-Pb hadron-to-pion ratios as a function of multiplicity normalised by the multiplicity-integrated ratio in pp, corresponding to the INEL>0 event class. While the p/π ratio stays practically constant, the increase of strange and multi-strange obeys a clear hierarchy with the strangeness content. PYTHIA8 [17] cannot reproduce the observed enhancement with multiplicity in pp. DIPSY [24] and EPOS LHC [11] predict a rising trend with multiplicity but miss the magnitude of the ratio

and the flat trend of p/π .

Studies on multiplicity dependence of identified particle production continue on the data of pp collisions at $\sqrt{s} = 13$ TeV collected during the Run II of the LHC. An open question is whether the observed trend continues even further with multiplicity or if, instead, the strange to non-strange production saturates. In order to address this question, ALICE has collected a data sample with dedicated triggers to select high-multiplicity proton-proton events, that are being analysed at the moment of writing. The first results in minimum bias pp collisions at $\sqrt{s} = 13$ TeV show that the average charged particle multiplicity increases by about 15% from 7 TeV to the new collision energy [25]. No dependence on \sqrt{s} is observed in the differential and integrated K/π ratio, nor for the integrated K^{*0}/K and ϕ/K ratios, continuing the trend from lower to LHC energies. Instead, Ξ/π and Ω/π exhibit a small increase from inelastic collisions at $\sqrt{s} = 7$ TeV to $\sqrt{s} = 13$ TeV. Whether this increase can be described as being only a consequence of the higher average multiplicity that is attained at the higher collision energy is a question that will be addressed with a multiplicity-differential study based on the 13 TeV data.

5. Outlook and conclusions

Several new ALICE results have been presented at this conference, including the preliminary measurements of the nuclear modification factor of charged particles in Pb–Pb collisions at $\sqrt{s_{NN}} = 5.02$ TeV and the measurements of the production of a comprehensive set of identified particles with different strangeness content. The results in pp collisions have revealed interesting features that are similar to those observed in p–Pb and Pb–Pb. While these features are usually interpreted as due to collectivity in Pb–Pb collisions, their origin in smaller systems is still to be fully understood (radial flow, color reconnection...). An enhancement of strangeness production has been observed towards high-multiplicity pp with respect to inelastic events, that is not satisfactorily explained by QCD-inspired models available. The analysis of the data collected in the LHC Run II at the highest collision energy ever reached in a collider may shed more light on the energy and multiplicity evolution of strangeness production.

References

- [1] Rafelski J and Müller B 1982 *Phys. Rev. Lett.* **48**(16) 1066–1069
- [2] Khachatryan V *et al.* (CMS) 2010 *JHEP* **09** 091
- [3] Abelev B *et al.* (ALICE) 2013 *Phys.Lett.* **B719** 29–41
- [4] Abelev B B *et al.* (ALICE Collaboration) 2014 *Int. J. Mod. Phys.* **A29** 1430044
- [5] Adam J *et al.* (ALICE Collaboration) 2016 *Phys. Rev.* **C93** 034913
- [6] Abelev B B *et al.* (ALICE Collaboration) 2015 *Phys. Rev.* **C91** 024609
- [7] Gronefeld J M (ALICE Collaboration) 2016 *PoS (LHCP2016)* 126
- [8] Adam J *et al.* (ALICE) 2016 *Phys. Lett.* **B760** 720–735
- [9] Colella D (ALICE Collaboration) 2016 *these proceedings*
- [10] Adam J *et al.* (ALICE) 2016 *Eur. Phys. J.* **C76** 245
- [11] Pierog T, Karpenko I, Katzy J M, Yatsenko E and Werner K 2015 *Phys. Rev.* **C92** 034906
- [12] Minissale V, Scardina F and Greco V 2015 *Phys. Rev.* **C92** 054904
- [13] Souza R D D (ALICE Collaboration) 2016 *these proceedings*
- [14] Schnedermann E, Sollfrank J and Heinz U W 1993 *Phys. Rev.* **C48** 2462–2475
- [15] Abelev B *et al.* (ALICE Collaboration) 2013 *Phys.Rev.* **C88** 044910
- [16] Bierlich C and Christiansen J R 2015 *Phys. Rev. D* **92**(9) 094010
- [17] Sjostrand T, Mrenna S and Skands P Z 2008 *Comput. Phys. Commun.* **178** 852–867
- [18] Bleicher M and Aichelin J 2002 *Phys. Lett.* **B530** 81–87
- [19] Knospe A (ALICE Collaboration) 2016 *these proceedings*
- [20] Knospe A G, Markert C, Werner K, Steinheimer J and Bleicher M 2016 *Phys. Rev.* **C93** 014911
- [21] Stachel J, Andronic A, Braun-Munzinger P and Redlich K 2014 *J. Phys. Conf. Ser.* **509** 012019
- [22] Cleymans J, Kraus I, Oeschler H, Redlich K and Wheaton S 2006 *Phys. Rev.* **C74** 034903
- [23] Adam J *et al.* (ALICE) 2016 (*Preprint 1606.07424*)
- [24] Bierlich C, Gustafson G, Lönnblad L and Tarasov A 2015 *JHEP* **03** 148
- [25] Adam J *et al.* (ALICE Collaboration) 2016 *Phys. Lett.* **B753** 319–329